



Research paper

Structural design and simulation analysis of large permeable parking lot in sponge city based on SWMM

Chaoqin Bai¹, Yibo Wang²

Abstract: To improve the safety of urban underground parking lot and promote the construction of sponge city, a large parking lot structure of sponge city was designed based on rainstorm water management model (SWMM). A new permeable material paving method was designed for a parking lot in Handan City, and a low impact development (LID) parking lot model was constructed based on the SWMM. The simulation results showed that the runoff reduction effect of the permeable parking lot was significant. There was a delay of 3.36 minutes during the 30 minutes of rainfall period. During the 60 minutes rainfall period, there was a delay of 8.5 minutes. The lowest runoff reduction rate was 44% for a 100-year return period. The highest runoff reduction rate was 100% for 60 minutes rainfall duration and a 1-year return period. The lowest runoff reduction rate was 50% for a 100-year return period. The LID permeable parking lot had better runoff control effect, with a total runoff volume of 233 m³, a reduction rate of 83.5%, a peak flow rate of 0.152 m³/s, and a reduction rate of 73.4%. The LID parking lot model developed based on the SWMM has better drainage and water storage performance, making it more suitable for the construction of large permeable parking lots in sponge cities. The permeable parking lot structure studied effectively reduces the time of runoff effect of parking lot, improves the safety of underground parking lot during rainstorm, and promotes the construction and development of sponge city.

Keywords: SWMM, LID, permeable parking lot, runoff control, hydrological characteristics

¹Assoc Prof., MSc., School of Civil Engineering and Architecture, Henan University of Science and Technology, Luoyang, 471000, China, e-mail: 9903255@haust.edu.cn, ORCID: 0009-0001-6521-7791

²MSc., School of Civil Engineering and Architecture, Henan University of Science and Technology, Luoyang, 471000, China, e-mail: alex_adelaide@163.com, ORCID: 0009-0004-7137-0428

1. Introduction

Since the reform and opening up in 1978, China's urbanization process has shown a rapid development momentum. With the advancement of urbanization, the mode of transportation is gradually shifting from walking and public transportation to self driving or private cars, and the proportion is constantly increasing [1]. In the early stages of urbanization construction in China, to meet the needs of rapid urban development, most urban infrastructure is built with impermeable materials such as cement and asphalt. Especially in the construction of large parking lots, impermeable materials are widely used to reduce costs and improve bearing capacity. However, this approach has brought serious environmental problems. Impermeable materials are widely used, resulting in the inability of urban surface water to penetrate and hindering the exchange of water vapor between soil and air [2]. The intensive urban construction and impermeable materials such as cement and asphalt have increased the city's heat absorption and storage capacity. The commonly used permeable pavement method cannot meet the bearing capacity requirements of parking lots, resulting in many large parking lots still using reinforced cement concrete with good bearing capacity for construction. To alleviate the urban heat island effect and build sponge city construction, a parking lot permeable material pavement method based on Storm Water Management Model (SWMM) is proposed. A parking lot model for Low Impact Development (LID) is constructed. The innovation of the research lies in the design of a permeable material paving method for underground parking lots, achieving sponge city construction and increasing the load of underground parking lots.

2. Related works

With the continuous development of urbanization, urban ecological problems are being paid more attention. To improve the service life of permeable concrete in urban construction, Aravind and Abdulrehman reinforced it based on a ratio of 1% aluminum powder and 15% fly ash. In the compressive strength and infiltration tests, the average compressive strength was 12.9% higher, but the infiltration rate was 25.6% lower [3]. Tirpak et al. tested a parking lot with pervious concrete pavement in Ohio. The observed data was used for SWMM modeling. Compared with completely impervious parking lots, the cumulative runoff of the SWMM decreased by 43%, and the median peak flow decreased by 75%. The peak flow reduction only applied to non flood events [4]. Chen et al. selected a large parking lot in Xi'an and conducted attenuation experiments with different structures. The results indicated that the permeable surface blockage went through three stages: rapid blockage, local blockage, and gradual blockage. Permeable cotton was more prone to clogging during parking [5]. Liu et al. proposed an innovative permeable pavement with capillary columns and water storage areas inside. The results showed that the new material was more effective in alleviating the urban heat island effect. The maximum surface temperature of the innovative permeable pavement test zone decreased by about 15°C lower in the hot summer [6]. Zhang et al. constructed two permeable parking lots and one impermeable concrete pavement in Shanghai to investigate the hydrological characteristics of permeable interlocking concrete pavements with distinct base

materials. The results showed that the capacity reduction rates of the two permeable parking lots were 37.0% and 38.7%. The peak flow reduction rate and peak arrival time of the two parking lots were better than those of the impermeable roads [7].

To reduce the impact of urbanization and industrialization on urban hydrological characteristics, Lee et al. constructed a LID model using SWMM software. The results showed that LID model can reduce 10% of storm water runoff and 15% of pollutants such as suspended solids from road surfaces [8]. To evaluate the performance of green roofs in urban SWMM, Paithankar and Taji selected some areas to install green roofs. The results showed that installed green roof reduced the peak flow in the area by 770 mm/s. Integrated green roofs could reduce rainwater runoff [9]. Ajibade, et al, developed a new decentralized sustainable camp drainage system to deal with storm water problems in refugee camps in Kenya. The SWMM was used for modeling and simulation. The results showed that it could handle the expected peak flow and total net flow [10]. To assess the accuracy of SWMM simulation capability, Platz et al. used a multi-event, multi-objective calibration approach to quantitatively compare empirical data with model results. The results showed that SWMM accurately simulated 90% of the target hydrological characteristics [11].

In summary, there are many aspects that can be improved in the surface laying of permeable materials, but currently most improvement methods sacrifice the permeability of the material. Therefore, this study combines existing information to improve the paving of permeable surfaces, maximizing their permeability while greatly enhancing their bearing capacity. Moreover, the LID model constructed by SWMM software has received better evaluation in hydrological characteristics research. Therefore, this paper applies this method to evaluate the proposed permeable structure.

3. The design of permeable parking structure based on SWMM

3.1. Structural design of permeable parking lots

The traffic volume, traffic composition and bearing capacity of the area are mainly considered in the design of the conventional parking lot, which will lead to the risk of flooding of the underground parking lot in rainstorm. If the hydrological characteristics of the parking lot are fully considered during construction, it can effectively avoid the risk of flooding. Therefore, based on the rainfall characteristics of Handan City, this study analyzes the hydrological characteristics of permeable parking lots through artificial simulation of rainfall. The rainfall in permeable parking lots is partly for wetting materials, and partly for the accumulation of water pits. Runoff only occurs when the rainfall intensity is greater than the permeability of the material and continuous rainfall occurs. The delay time of runoff can be calculated using Formula (3.1) [12].

$$(3.1) \quad I \times T_e = (X_t + S_d) + K \times T_e$$

In Formula (3.1), T_e is the runoff delay time. I is the rainfall intensity. X_t is the plant interception. S_d is the pond storage. K is the infiltration coefficient. If the calculation area

consists of permeable and impermeable areas, then the initial rainfall loss should be calculated according to the impermeable and permeable areas. Formula (3.1) can be rewritten as Formula (3.2).

$$(3.2) \quad T_e = \frac{0.5L_p A_p + L_i A_i}{IA - K A_p}$$

In Formula (3.2), A_p is the permeable pavement area. A_i is the impervious pavement area. L_p is the initial loss of permeable pavement. L_i is the initial loss of impervious pavement. A is the total area. The runoff depth can be calculated using Formula (3.3).

$$(3.3) \quad R = I(T_d - T_e) - K(T_d - T_e)$$

In Formula (3.3), R is the runoff depth. T_d represents the duration of rainfall. $I(T_d - T_e)$ is the depth of rainfall after removing the initial loss. $K(T_d - T_e)$ is the permeability of the permeable road surface after generating runoff. Formula (3.3) can also be changed by permeable pavement and impermeable pavement, as shown in Formula (3.4).

$$(3.4) \quad R = (T_d - T_e) \left(1 - K \frac{A_p}{A} \right)$$

In Formula (3.4), if $A_i \times I \leq A_p(K - I)$, the pavement surface runoff will all be retained. At time R , if $A_i \times I > A_p(K - I)$, it means that the impervious pavement part of the runoff generated by the permeable pavement can be absorbed by the permeable pavement. At this time, it can be used to calculate the runoff depth of Formula (3.4). Therefore, the study uses general theoretical knowledge to estimate. The surface sheet flow prevalence time can be calculated using Manning variability formula, as shown in Formula (3.5) [13].

$$(3.5) \quad R = (T_d - T_e) \left(1 - K \frac{A_p}{A} \right)$$

In Formula (3.5), T_t is the confluence time. n represents the Manning roughness coefficient. L represents the confluence path length. P_2 is the 24-hour rainfall that occurs once every 2 years. S is the confluence path slope. Formula (3.5) can not only evaluate the peak runoff flow rate, but also change the parameters to study the key factors affecting the settlement time of permeable pavement. In the experiment, the rainwater infiltration intensity is set to $W(t)$. The rainwater infiltration intensity is $V(t)$. The unit area is combined with the water balance, as shown in Formula (3.6).

$$(3.6) \quad h(t) = \frac{1}{n_e} \int_0^t [W(t) - V(t)] dt$$

In Formula (3.6), n_e is the void ratio of the substrate material. t represents the rainfall calendar time. $h(t)$ represents the water storage height of the substrate at t . To simplify the calculation, the average rainfall intensity is used to calculate the rainfall. The permeable

pavement surface infiltration coefficient is greater than the rainfall intensity to ensure no runoff. The average rate of rainwater infiltration stage is used to calculate the infiltration time \bar{V} , as shown in Formula (3.7).

$$(3.7) \quad H = \left(0.1I - 3600\bar{V}\right) \frac{100T}{60n}$$

In Formula (3.7), H is the maximum value of $h(t)$ during the whole rainfall process. T is the time spent during the whole rainfall process. The calculation result of Formula (3.7) can be used as the control value of the structure thickness design. Similarly, the permeable pavement aquifer water completely infiltration time T_p is calculated, as shown in Formula (3.8).

$$(3.8) \quad T_p = \frac{1}{\bar{V}} [IT - H_b (n_f - n_0)]$$

In Formula (3.8), H_b is permeable pavement structure base thickness. n_f is the external water holding capacity. n_0 is the initial moisture content state. The T_p value can reflect the degree of damage caused by the internal moisture of the structure to the overall strength and stability.

3.2. Penetrable parking lot pavement design

SWMM is a sophisticated and sophisticated rainwater management simulation model that can simulate water movement within a watershed during and after precipitation events. They can predict runoff, time, and water quality entering receiving bodies such as rivers and lakes. By integrating hydrological, hydraulic, and water quality components, SMM provides a comprehensive analysis that helps decision-making in sustainable urban planning and environmental protection. With the advancement of technology, SWMM has become increasingly user-friendly and integrated with Geographic Information Systems (GIS) to enhance spatial analysis and visualization. Hebei is a region with heavy rainfall and frequent flooding disasters. Handan city is one of the areas with frequent heavy rainfall. To ensure that the permeable parking lot also has good permeability during the flood season, the thickness of the permeable base layer is calculated according to the rainfall conditions in Handan city. The permeable materials used in the construction of parking lots have been explained above. The rainfall intensity in Handan city is shown in Formula (3.9).

$$(3.9) \quad I_s = \frac{9.5336(1 + 0.5917 \lg p)}{(t + 5.9828)^{0.6383}}$$

In Formula (3.9), I_s represents the design storm intensity. p represents the recurrence period. t represents the rainfall calendar time. However, the commonly used permeable pavement currently adopts a brick pavement structure, which has poor bearing capacity and is prone to fatigue damage, resulting in structural layer damage. Therefore, the permeable layer pavement of the parking lot adopts a vegetation permeable structure pavement. The method not only improves the bearing capacity of the permeable layer, but also expands the urban greening area. The design method is shown in Fig. 1.

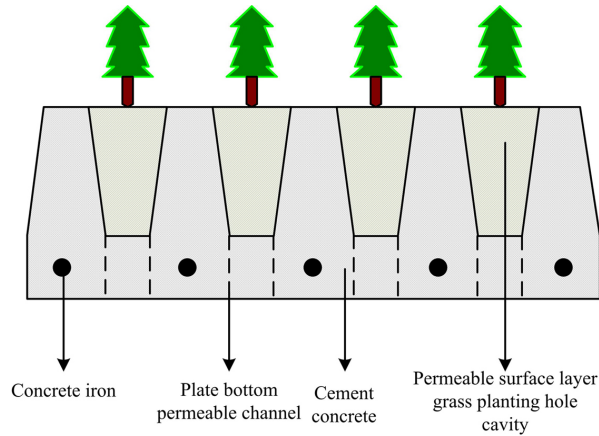


Fig. 1. Structural design of grassed permeable surface layer

This study designs a permeable parking lot with a surface concrete area of 47% and a hole area of 53%. Since the concrete is connected by steel reinforcement at the bottom, the structural integrity and load-bearing capacity is high. It is not damaged by water. In the material selection, factors such as vehicle type and the number of times the vehicle acts on the pavement need to be considered. Assuming a single axle with two 10kN wheels as the standard load, then the number of actions can be converted by Formula (3.10) [14].

$$(3.10) \quad N_s = \sum_{i=1}^n N_i \left(\frac{P_i}{10} \right)^{16}$$

In Formula (3.10), N_s is the number of actions. P_i is the total weight of axle loads for different axle types at i level. n is the number of axle types and axle load levels. N_i is the number of axle load actions for each type of i level. The study also designs the cumulative standard number of axle load actions within the year, as shown in Formula (3.11).

$$(3.11) \quad N_e = \frac{365N [(1 + \gamma)^f - 1]}{\gamma} \eta$$

In Formula (3.11), N_e is the cumulative number of standard axle load actions in the design year. f is the design year. N is the average daily standard axle load action in the first year after completion. γ is the average growth rate in the design year, and η is the wheel track lateral distribution coefficient. The structure of the studied and designed large planted fist water parking lot is shown in Fig. 2.

The runoff reduction effect is an indicator to assess the runoff control effect of permeable parking lots. Its total rate is calculated by Formula (3.12) [15].

$$(3.12) \quad \gamma = \frac{V_{\text{imp}} - V_p}{V_{\text{imp}}} \times 100\%$$

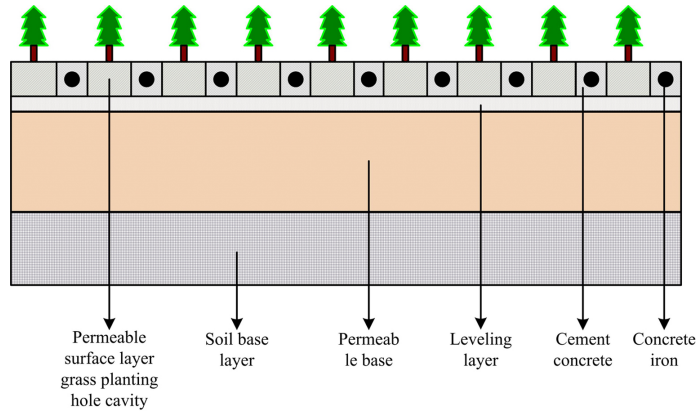


Fig. 2. Structural diagram of large grass planted fully permeable parking lot

In Formula (3.12), τ is the total runoff reduction rate. V_p is the total runoff from pervious parking lots. V_{imp} is the total runoff from impervious parking lots. q_{max} is the peak flow rate, as calculated by Formula (3.13).

$$(3.13) \quad \gamma = \frac{q_{max-imp} - q_{max-p}}{V_{max-imp}} \times 100\%$$

In Formula (3.13), γ is the peak flow reduction rate. q_{max-p} is the peak pervious parking lot flow. $q_{max-imp}$ is the peak impervious parking lot flow.

3.3. SWMM-based permeable parking structure design

SWMM is a comprehensive computer simulation model developed by the US Environmental Protection Agency (EPA) to simulate rainfall and surface runoff processes in urban areas and adjacent areas. The SWMM can be applied to single rainwater events or long-term (continuous) simulations, supporting the analysis of urban storm water discharge systems and LID measures. The study generalizes the target area with the principle of generalization, dividing the overall area into 12 sub-sink areas, two drainage pipe networks, and one drainage outlet. The delineation results are shown in Fig. 3 [16].

The selection and application of LID measures need to be initially screened based on the substrate type and landscape requirements of the renovation area. Then it is combined with the hydrological functions, construction and maintenance cost, and constraints of the LID facilities. Table 1 shows the hydrological functions and cost statistics of LID facilities [17].

In Table 1, "1", "2", and "3" indicate the lower, average, and higher levels, respectively. The SWMM constructed by the study mainly focuses the hydrological content of the LID model in the parking lot area. According to the runoff discharge system, the selection and layout of LID facilities are determined based on the hydrogeological conditions and rainfall runoff control objectives of Wei County, Handan city, in order to achieve integrated management of rainwater infiltration, accumulation, and discharge. The rainwater runoff path of the constructed SWMM is shown in Fig. 4.

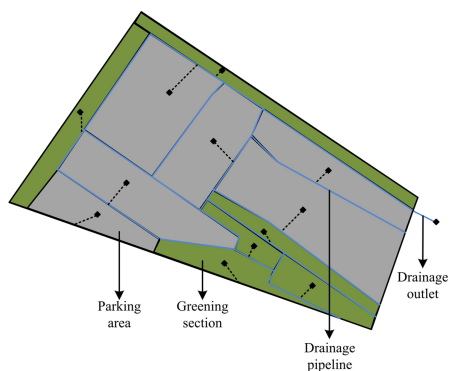


Fig. 3. Overview of the study area

Table 1. Hydrological function and cost statistics of LID facilities

LID measures	Function			Cost	
	Runoff reduction	Peak flow reduction	Replenishing groundwater	Construction cost	Maintenance cost
Grass planting ditch	2	2	2	2	1
Rainwater Garden	2	2	3	2	3
Permeable pavement	3	3	2	1	1
Green roof	2	2	1	2	3
Gravel system	2	3	2	2	2
Artificial wetland	3	2	2	3	2
Sunken green space	2	2	3	1	1

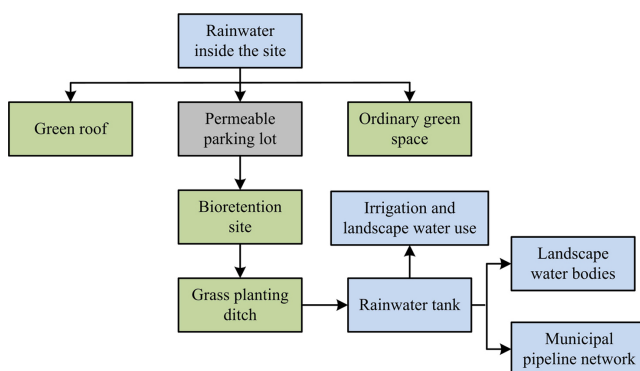


Fig. 4. SWMM rainwater discharge path diagram

It is difficult to ensure uniform rainfall intensity in actual rainfall. Therefore, in the rainfall design of rainwater management models, it is necessary to choose appropriate rainfall data. To maximally simulate the flood rainfall conditions in Handan city, the simulated rainfall process line is selected as the rainfall model. After designing the rainfall calculation, the time distribution of pre-peak rainfall can be calculated using Formula (3.14) [18, 19].

$$(3.14) \quad i(t_b) = \frac{a \left[\frac{(1-c)t_b}{r} + b \right]}{\left(\frac{t_a}{r} + b \right)^{1+c}}$$

In Formula (3.14), t_b is the pre-peak period. t_a is the post-peak period. $i(t_b)$ is the pre-peak rainfall intensity. a , b and c represent parameters. r is the rainfall peak coefficient. The post-peak rainfall time distribution can be calculated by Formula (3.15).

$$(3.15) \quad i(t_a) = \frac{a \left[\frac{(1-c)t_a}{r} + b \right]}{\left(\frac{t_a}{r} + b \right)^{1+c}}$$

In Formula (3.15), $i(t_a)$ is the post-peak rainfall intensity.

4. Simulation analysis of permeability effect in permeable parking lot construction

4.1. Permeable parking lots simulation results

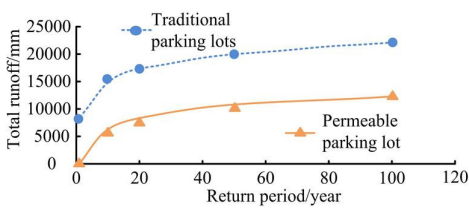
In the simulation test of permeable parking lot, artificially simulated rainfall is used for the research. Five different recurrence periods and three experimental groups are set up. Each experimental group has five rainfall intensities. Among which, the flow production time of ordinary parking lot is group A, and the flow production time of permeable parking lot is group B. The experimental results are shown in Table 2.

In Table 2, When the duration was 60 minutes, the average runoff occurrence time in permeable parking lots was 12.4 minutes, while in regular parking lots it was 3.9 minutes. Therefore, when the simulation experiment of runoff reduction effect was conducted, only the experimental groups of 30 minutes and 60 minutes were set. The results are shown in Fig. 5.

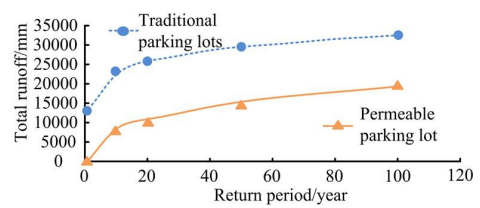
In Fig. 5, regardless of the rainfall duration of 30 minutes or 60 minutes, the total runoff of the permeable parking lot was always lower than the ordinary parking lot. In Fig. 5(a), the total runoff of the permeable parking lot increased from 1 to 100 with a rainfall duration of 30 minutes. The total runoff of the ordinary parking lot increased from 1 to 100 with an increase of 12,344 mm. In Fig. 5(c), the highest runoff reduction rate was 100% when the rainfall duration was 30 minutes. The data with a rainfall duration of 30 minutes is used to analyze the relationship between parking lot infiltration, runoff reduction rate, and return period. The results are shown in Table 3.

Table 2. Comparison of runoff time under different rainfall intensities

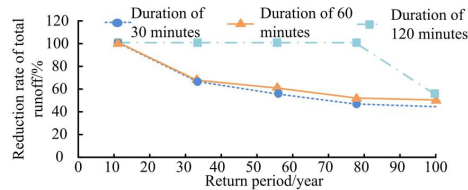
Return period	Rainfall for 30 minutes			Rainfall for 60 minutes			Rainfall for 120 minutes		
	Rainfall intensity	A	B	Rainfall intensity	A	B	Rainfall intensity	A	B
1	0.968	4.0	0.0	0.658	6.0	0	0.435	8.0	0
10	1.541	2.0	9.0	1.047	3.8	19	0.693	5.7	0
20	1.714	1.6	7.0	1.164	3.6	17	0.770	5.0	0
50	1.942	1.1	5.5	1.319	3.2	14	0.873	4.0	0
100	2.114	0.6	4.6	1.436	2.9	12	0.950	3.3	17



(a) 30 minute rainfall duration parking lot runoff



(b) 60 minute rainfall duration parking lot runoff



(c) Comparison of total runoff reduction rates

Fig. 5. Comparison of runoff reduction effects in parking lots

Table 3. Data analysis for rainfall duration of 30 minutes

Return period	1	10	20	50	100
Water inflow	12269	19532	21725	24615	26795
Infiltration amount	12269	13533	13957	14312	14450
Runoff	0	5199	7368	10303	12345
Reduction rate of total runoff	100	66	56	48	44

In Table 3, the total runoff reduction rate was 34% when the recurrence period was 1–10 years. Then the reduction rate of total net flow began to stabilize and flatten. From 10–100 years, the total reduction rate of runoff reduced by 22%. The research suggests that the runoff reduction in permeable parking lots mainly depends on the absorption and infiltration capacity of the permeable surface and storage structure. When the rainfall exceeded the overall capacity of the parking lot, the runoff reduction rate started to decrease.

4.2. SWMM-based simulation analysis of permeable parking lots

The artificial simulated rainfall line in the SWMM is the Chicago rainfall hydrograph model. The simulation experiment selects parameters with a return period of 1 to 100, with rainfall duration ranging from 1 minute to 180 minutes. The calculated rainfall time distribution under these parameters is shown in Fig. 6.

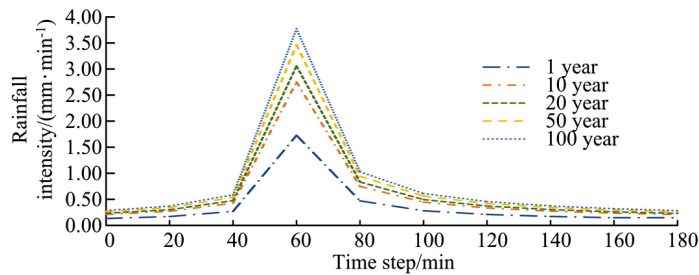


Fig. 6. Rainfall time history distribution under different return periods

In Fig. 6, the rainfall peaks were at 60 minutes of rainfall time, with the peak of 1.7276 for 1-year return period, 2.7498 for 10-year, 3.0575 for 20-year, 3.4643 for 50-year, and 3.7720 for 100-year. As return period increases, the duration peak also increases. At each return period, the rainfall duration crossed the peak and then started to decrease. At 180 minutes, all rainfall duration decreased to the level at the beginning. In the operation of the SWMM in Handan city, parameters with a 20-year return period and a 50-year return period are selected for simulation experiments. The results are shown in Fig. 7.

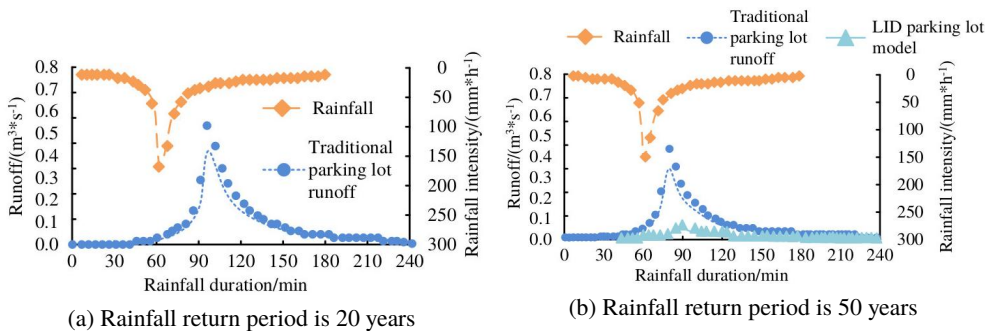
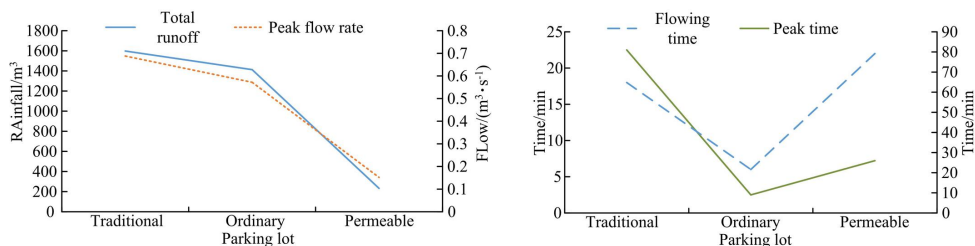


Fig. 7. Curve chart of runoff regulation and storage effect between traditional parking lot model and LID development model

In Fig. 7(a), the maximum rainfall reached 190 mm/h at the rainfall ephemeris of 60 minutes for a rainfall return period of 20 years. The runoff volume of the conventional parking lot model reached the maximum of 0.522 m³/s at the rainfall ephemeris of 95 minutes. The runoff volume of the LID model was 0 for a rainfall return period of 20 years. Compared with the LID model, the peak runoff volume of the conventional parking lot model was 0.522 m³/s

higher than that of the LID model. In Fig. 7(b), the maximum rainfall volume was 200 mm/h at 60 minutes. The peak runoff volume of the conventional parking lot model was $0.688 \text{ m}^3/\text{s}$ at 81 minutes. The peak runoff volume of the LID model was $0.583 \text{ m}^3/\text{s}$ higher than the LID model. To compare the effect gap between the permeable parking lot and the traditional parking lot, the simulation is conducted under a 1-year rainfall return period and a 3-hour rainfall duration. The results are shown in Fig. 8.



(a) Comparison of total net flow and peak flow in different parking lots (b) Comparison of runoff time and reduction in different parking lots

Fig. 8. Comparison of water permeability of different parking lots

In Fig. 8, for a 50-year return period, the permeable parking lot had a runoff reduction of 1180 m^3 , while the ordinary parking lot had no runoff reduction. The permeable parking lot exhibited a total runoff reduction of 83.5%. Its peak flow rate was $0.152 \text{ m}^3/\text{s}$, while the ordinary parking lot was $0.572 \text{ m}^3/\text{s}$. Consequently, the permeable parking lot had a peak reduction of $0.42 \text{ m}^3/\text{s}$, and its peak flow reduction rate reached 73.4%. The flow production time of the permeable parking lot started at 22 minutes.

4.3. Conclusions

To study the hydrological characteristics based on SWMM, this research took the parking lot of Weizi Park in Handan city as the research object. The LID permeable parking lot model based on SWMM was designed. The model was subjected to simulation experiments. The simulation experiment results showed that the runoff reduction effect of the permeable parking lot was more obvious. The runoff reduction rate of the permeable parking lot meets the requirements. Among the three ephemeris conditions in the study, the runoff reduction rate of the permeable parking lot was the lowest at 44% and the highest at 100%. The LID parking lot model showed significant runoff. No runoff occurred in the LID model with a rainfall return period of 20 years. For the 50-year rainfall return period, the LID model showed runoff, which reached a peak runoff rate of $0.105 \text{ m}^3/\text{s}$ at 90 minutes of rainfall. The total runoff reduction rate was 83.5%. The peak flow reduction rate was 73.4%. The experiment verifies that the permeability performance is better under the SWMM. However, due to the limited experimental conditions, many aspects need to be carefully optimized.

References

- [1] S. Arshad, S.R. Ahmad, S. Abbas, et al., “Quantifying the contribution of diminishing green spaces and urban sprawl to urban heat island effect in a rapidly urbanizing metropolitan city of Pakistan”, *Land Use Policy*, vol. 113, no. 1, art. no. 105874, 2022, doi: [10.1016/j.landusepol.2021.105874](https://doi.org/10.1016/j.landusepol.2021.105874).
- [2] V.I. Vasenev, M. Varentsov, P. Konstantinov, et al., “Projecting urban heat island effect on the spatial-temporal variation of microbial respiration in urban soils of Moscow megalopolis”, *Science of The Total Environment*, vol. 786, no. 2, 2021, doi: [10.1016/j.scitotenv.2021.147457](https://doi.org/10.1016/j.scitotenv.2021.147457).
- [3] N. Aravind and T.I. Abdulrehman, “A review and sequel experimental analysis on physical and mechanical properties of permeable concrete for pavement construction”, *International Journal of Pavement Engineering*, vol. 23, no. 12, pp. 4160–4173, 2022, doi: [10.1080/10298436.2021.1936519](https://doi.org/10.1080/10298436.2021.1936519).
- [4] A. Tirpak, R.J. Winston, M. Feliciano, et al., “Impacts of permeable interlocking concrete pavement on the runoff hydrograph. Volume reduction, peak flow mitigation, and extension of lag times”, *Hydrological Processes*, vol. 35, no. 4, pp. 1–14, 2021, doi: [10.1002/hyp.14167](https://doi.org/10.1002/hyp.14167).
- [5] W. Chen, M.L. Zheng, Q. Gao, and C.X. Deng, “Attenuation law of permeable pavement in sponge city. Chang’an Daxue Xuebao (Ziran Kexue Ban)”, *Journal of Chang’an University (Natural Science Edition)*, vol. 41, no. 3, pp. 12–21, 2021, doi: [10.19721/j.cnki.1671-8879.2021.03.002](https://doi.org/10.19721/j.cnki.1671-8879.2021.03.002).
- [6] Y. Liu, T. Li, and L. Yu, “Urban heat island mitigation and hydrology performance of innovative permeable pavement: a pilot-scale study”, *Journal of Cleaner Production*, vol. 244, art. no. 118938, 2020, doi: [10.1016/j.jclepro.2019.118938](https://doi.org/10.1016/j.jclepro.2019.118938).
- [7] J.W. Zhang, Y. Liu, J.R. Jin, and T. Li, “Performance assessment of permeable interlocking concrete pavement facility structure”, *Huanjing Kexue*, vol. 41, no. 2, pp. 750–755, 2020, doi: [10.13227/j.hj.kx.201908085](https://doi.org/10.13227/j.hj.kx.201908085).
- [8] H. Lee, W. Woo, and Y.S. Park, “A user-friendly software package to develop Storm Water Management Model (SWMM) inputs and suggest low impact development scenarios”, *Water*, vol. 12, no. 9, art. no. 2344, 2020, doi: [10.3390/w12092344](https://doi.org/10.3390/w12092344).
- [9] D. Paithankar and S. Taji, “Investigating the hydrological performance of green roofs using storm water management model”, *Materials Today: Proceedings*, vol. 32, no. 4, pp. 943–950, 2020, doi: [10.1016/j.matpr.2020.05.085](https://doi.org/10.1016/j.matpr.2020.05.085).
- [10] O.O. Ajibade, K. Tota-Maharaj, C.D. Hills, and C. Macleod, “Modelling of a sustainable refugee camp drainage system for stormwater management”, *Environmental Science: Water Research and Technology*, vol. 5, no. 12, pp. 2150–2161, 2019, doi: [10.1039/C9EW00350A](https://doi.org/10.1039/C9EW00350A).
- [11] M. Platz, M.A. Simon, and M. Tryby, “Testing of the storm water management model low impact development modules”, *Jawra Journal of the American Water Resources Association*, vol. 56, no. 2, pp. 283–296, 2020, doi: [10.1111/1752-1688.12832](https://doi.org/10.1111/1752-1688.12832).
- [12] J.H. Diaz-Hernandez and A.J. Herrera-Martinez, “Hydrological characteristics and paradoxes of mediterranean high-mountain water-bodies of the Sierra -Nevada, SE Spain”, *Hydrology*, vol. 6, no. 3, pp. 59–78, 2019, doi: [10.3390/hydrology6030059](https://doi.org/10.3390/hydrology6030059).
- [13] H. Zhang, Z. Wang, W. Xu, and H. Wang, “Determination of emergent vegetation effects on manning’s coefficient of gradually varied flow”, *IEEE Access*, vol. 7, no. 11, pp. 146778–146789, 2019, doi: [10.1109/ACCESS.2019.2946917](https://doi.org/10.1109/ACCESS.2019.2946917).
- [14] F. Abbondati, S.A. Biancardo, R. Veropalumbo, and G. Dell’Acqua, “Surface monitoring of road pavements using mobile crowdsensing technology”, *Measurement*, vol. 171, no. 11, pp. 108763–108771, 2021, doi: [10.1016/j.measurement.2020.108763](https://doi.org/10.1016/j.measurement.2020.108763).
- [15] J. Peng, X. Zhong, L. Yu, and Q. Wang, “Simulating rainfall runoff and assessing LID facilities in sponge airport”, *Water Science and Technology*, vol. 82, no. 5, pp. 918–926, 2020, doi: [10.2166/wst.2020.400](https://doi.org/10.2166/wst.2020.400).
- [16] A. Damseaux, X. Fettweis, M. Lambert, and Y. Cornet, “Representation of the rain shadow effect in Patagonia using an orographic-derived regional climate model”, *International Journal of Climatology*, vol. 40, no. 3, pp. 1769–1783, 2020, doi: [10.1002/joc.6300](https://doi.org/10.1002/joc.6300).
- [17] W. Yang, J. Zhang, and P. Krebs, “Low impact development practices mitigate urban flooding and non-point pollution under climate change”, *Journal of Cleaner Production*, vol. 347, 2022, doi: [10.1016/j.jclepro.2022.131320](https://doi.org/10.1016/j.jclepro.2022.131320).
- [18] E. Khaleghi, A. Sadoddin, A. Najafinejad, and A. Bahremand, “Flood hydrograph simulation using the SWMM model: a semiarid zone watershed case study, Shiraz Khoshk River, Iran”, *Natural Resource Modelling*, vol. 33, no. 2, pp. 12269–12280, 2020, doi: [10.1111/nrm.12269](https://doi.org/10.1111/nrm.12269).

- [19] E. Szczepański, M. Jacyna, R. Jachimowski, R. Vašek, and K. Nehring, “Decision support for the inter-modal terminal layout designing”, *Archives of Civil Engineering*, vol. 67, no. 2, pp. 611–630, 2021, doi: [10.24425/ace.2021.137188](https://doi.org/10.24425/ace.2021.137188).

Received: 2024-03-18, Revised: 2024-06-27